J Membrane Biol (2015) 248:197–204
DOI 10.1007/s00232-014-9757-6

Docetaxel Modulates the Delayed Rectifier Potassium Current (I_K) and ATP-Sensitive Potassium Current (I_{KATP}) in Human Breast Cancer Cells

Tao Sun · Zhi-Guo Song · Da-Qing Jiang · Hong-Guang Nie · Dong-Yun Han

Received: 15 July 2013 / Accepted: 25 July 2014 / Published online: 25 November 2014

Abstract Ion channel expression and activity may be affected during tumor development and cancer growth. Activation of potassium (K^+) channels in human breast cancer cells is reported to be involved in cell cycle progression. In this study, we investigated the effects of docetaxel on the delayed rectifier potassium current (I_K) and the ATP-sensitive potassium current (I_{KATP}) in two human breast cancer cell lines, MCF-7 and MDA-MB-435S, using the whole-cell patch-clamp technique. Our results show that docetaxel inhibited the I_K and I_{KATP} in both cell lines in a dose-dependent manner. Compared with the control at a potential of +60 mV, treatment with docetaxel at doses of 0.1, 1, 5, and 10 μM significantly decreased the I_K in MCF-7 cells by 16.1 ± 3.5, 30.2 ± 5.2, 42.5 ± 4.3, and 46.4 ± 9 % ($n = 5$, $P < 0.05$), respectively and also decreased the I_{KATP} at +50 mV. Similar results were observed in MDA-MB-435S cells. The *G–V* curves showed no significant changes after treatment of either MCF-7 or MDA-MB-435S cells with 10 μM docetaxel. The datas indicate that the possible mechanisms of I_K and I_{KATP} inhibition by docetaxel may be responsible for its effect on the proliferation of human breast cancer cells.

Keywords Docetaxel · Patch-clamp technique · Breast cancer · Potassium channels

Introduction

Potassium channels (K^+ channels) comprise the largest and most diverse family of plasma membrane channels. K^+ channels have essential functions in all cell types, but their extreme diversity confers K^+ channels with great functional variability (Hille 1992; Wonderlin and Strobl 1996; Leanza et al. 2014). Tumorigenesis is a complicated process, involving a series of genetic alterations and signal transduction pathways. Ion channel expression and activity may be affected during tumor development and growth of cancer, along with many other changes. The roles of ion channels in the proliferation and development of cancer have been recently reported. In particular, activation of K^+ channels is crucial for progression through the G1 phase of the cell cycle (Wonderlin and Strobl 1996; Mound et al. 2013).

Investigation of the functional properties of K^+ channels in cancer cells is emerging as a novel approach for the development of anticancer therapeutics. It has been reported that regulation of K^+ channel activity may

Tao Sun and Zhi-Guo Song made equal contributions to this study.

T. Sun (✉)
Department of Internal Oncology, Liaoning Cancer Hospital and Institute, Shenyang 110042, China
e-mail: jianong@126.com

Z.-G. Song
Department of Pharmacology, School of Pharmacy, China Medical University, Shenyang 110001, China

D.-Q. Jiang
Department of Breast Oncology, Liaoning Cancer Hospital and Institute, Shenyang 110042, China

H.-G. Nie
Laboratory of Metabolic Disease Research and Drug Development, China Medical University, Shenyang 110001, China

D.-Y. Han
Department of Physiology and Biophysics, Case Western Reserve University School of Medicine, Cleveland, OH 44106, USA

contribute to the inhibition of breast cancer cell proliferation (Wonderlin and Strobl 1996). In previous electrophysiological studies, at least four types of K^+ current that are active in human breast cancer MCF-7 cells were identified. Each displays different sensitivities to voltage, intracellular Ca^{2+}, or ATP: (i) the Ca^{2+}-activated K^+ current ($I_{K\cdot Ca}$) (Wegman et al. 1991), (ii) the ATP-sensitive K^+ current (I_{KATP}) (Klimatcheva and Wonderlin 1999), (iii) the delayed rectifier K^+ current (I_K) (Ouadid-Ahidouch et al. 2000), and (iv) the EAG K^+ current (I_{EAG}) (Ouadid-Ahidouch et al. 2001). Because the activity of K^+ channels is closely correlated with cell proliferation in breast cancer cells, K^+ channels can be considered a potential pharmacological target for cancer treatment.

Docetaxel, a semi-synthetic compound, is produced from a natural product 10-deacetylbaccatin-III that can be collected from the needles of the European yew tree, *Taxus baccata* (Gelmon 1994). In recent years, docetaxel has become one of the most important novel chemotherapeutic agents used clinically. Studies on docetaxel found that it can stabilize tubulin by inhibiting the dynamic reorganization of the microtubular network of the cell, leading to inhibition of mitotic and interphase cellular functions (Schiff et al. 1979; Dyrager et al. 2011). In addition to its effects on microtubules, docetaxel also appears to have functions related to the inhibition of tumor cell growth (Yasumizu et al. 2014). However, the ionic mechanism underlying the inhibition of cancer cell proliferation has not yet been fully elucidated. The present study aimed to identify the electrophysiological characteristics of K^+ channels in human breast cancer cells, particularly focused on the effects of docetaxel on the I_K and I_{KATP} in the MCF-7 and MDA-MB-435S cell lines, using patch-clamp techniques under the standard whole-cell configuration.

Materials and Methods

Cell Preparation

MCF-7 and MDA-MB-435S cells were cultured in RPMI 1640 medium (Life Technologies, Inc. Crand Island, NY), supplemented with 10 % heat-inactivated fetal bovine serum (Hyclone laboratories, Inc., Logan, UT), and maintained at 37 °C in a humidified atmosphere of 95 % air/5 % CO_2. For patch-clamp recordings at the single-cell level, cells were plated onto 35 mm dishes at a density of 10^4 cells/cm^2.

Reagents

Docetaxel was purchased from Aventis Pharma (Dagenham, France). Prior to the experiment, docetaxel solutions of different concentrations were prepared in distilled water and added separately to the different baths. Tetraethylammonium chloride (TEA), 4-aminopyridine (4-AP), and glibenclamide were purchased from Sigma. TEA and 4-AP were prepared as 0.1 M stock solutions in distilled water; glibenclamide was dissolved in dimethylsulfoxide (DMSO) to prepare a 1 mM stock solution.

Pipette Solutions

Cells were perfused with an external physiological solution containing (in mM): 143 NaCl, 5.4 KCl, 0.5 $MgCl_2$, 1.8 $CaCl_2$, 0.3 NaH_2PO_4, 2.3 NaOH, 5 D-glucose, and 5 HEPES at pH 7.4 (adjusted with NaOH). For I_K recordings, patch pipettes were filled with a solution containing (in mM): 135 KCl, 10 EGTA, 5 Na_2ATP, 5 D-glucose, and 10 HEPES at pH 7.2 (adjusted with KOH). For I_{KATP} recordings, patch pipettes were filled with a solution containing (in mM): 143 NaCl, 5.4 KCl, 0.5 $MgCl_2$, 0.3 Na_2 ATP, and 5 EGTA at pH 7.2 (adjusted with KOH).

Electrophysiology

Whole-cell patch-clamp recording was carried out on single cells at room temperature ($\sim$18–20 °C). Measurements of membrane currents were performed in the standard whole-cell patch-clamp configuration with an Axopatch-1D amplifier (Axon Instruments, USA). Patch electrodes were pulled with a two-stage vertical puller (PP-83, Narishige, Japan) and verified within a resistance range of 3–5 MΩ. Membrane potential and currents were monitored with a dual-beam memory oscilloscope (VC-10, Nihon Kohden, Japan). Data for each sample were collected with an AD/DA converter (Digidata 1200, USA) and stored electronically. Series resistance and capacitance transients were compensated with an Axopatch-1D amplifier. For I_K recordings, the voltage-clamp protocol was as follows: membranes were held at −90 mV, the step pulse was 10 mV, the test potential was −90 to +60 mV, the duration was 200 ms, and the interval between stimulations was 3 s. For I_{KATP} recordings, membranes were held at −40 mV, the step pulse was 10 mV, the test potential was −100 to +50 mV, and the duration was 300 ms. Pulses were applied every 3 s. The leak currents were subtracted from all recordings.

Statistics

Data analysis was performed using pCLAMP 5.5.1 software (Axon Instruments). The I_K and I_{KATP} were measured as the amplitude of the current remaining at the end of the test pulse relative to the zero current level. Data were presented as mean ± standard error (SE). Student's *t* test

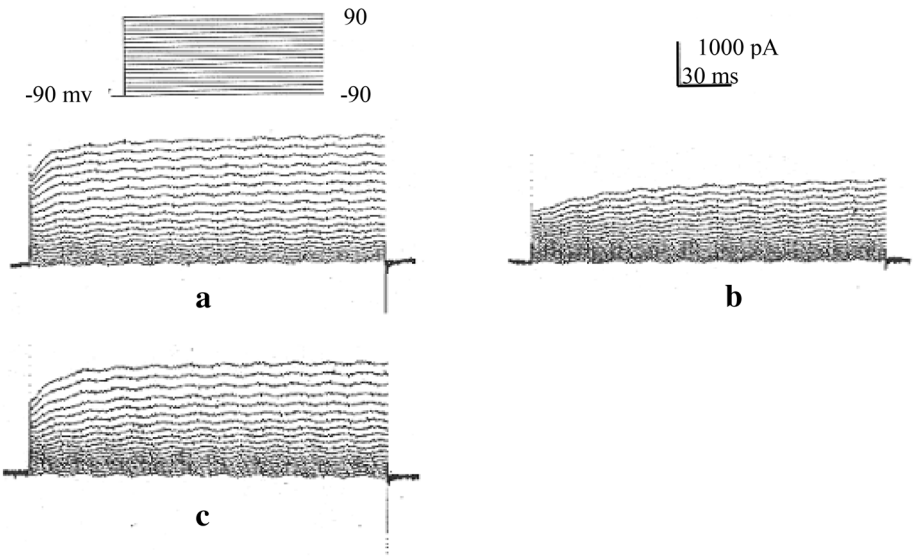

Fig. 1 The effect of TEA on the I_K in MCF-7 cells. **a** Control; **b** Perfusion with TEA; **c** 5 min after washout

was used to determine the statistical significance of sample testing, and values of $P < 0.05$ were considered significant.

Results

Comparison of I_K Measurements Between MCF-7 and MDA-MB-435S Cells

Whole-cell patch-clamp experiments were performed on single cells in culture dishes. To block Ca^{2+} and Na^{+} currents, cells were pre-treated with verapamil (1 μM) and tetrodotoxin (0.1 μM), respectively, added to the extracellular solution. In our study, outward currents were detected in both MCF-7 and MDA-MB-435S cells under the voltage-clamp mode using a series of 200 ms voltage pulses from −90 to +60 mV in 10 mV increments, from a holding potential of −90 mV. Meanwhile, pulses were applied every 3 s.

As the control, the effect of TEA on outward K^{+} currents in MCF-7 cells was evaluated first. The recording confirmed that extracellular perfusion with 10 mM TEA reduced the current amplitude. At +60 mV potential, the inhibitory rate of TEA on outward currents was approximately 27 %. However, this inhibition by TEA could be reversed in MCF-7 cells by a washout with an external physiological solution (Fig. 1). The current amplitude at +60 mV potential was also reduced by approximately 46 % in MCF-7 cells after perfusion with 10 mM 4-AP. Similar effects of TEA and 4-AP on outward currents were also observed in MDA-MB-435S cells (data not shown). These results indicate that outward currents in MCF-7 and MDA-MB-435S cells are carried primarily by K^{+} ions.

The I_K values measured in MCF-7 and MDA-MB-435S cells were activated by a long depolarization pulse beyond approximately −80 mV. In similar experiments, we observed that if the potential was higher than −30 mV, the amplitudes of the I_K in MCF-7 cells were much larger than those in MDA-MB-435S cells ($P < 0.01$; data not shown).

Comparison of I_{KATP} Measurements Between MCF-7 and MDA-MB-435S Cells

In the whole-cell configuration, outward currents were measured by applying voltage steps (−100 to +50 mV) from the holding potential of −40 mV. Outward currents were recorded in both MCF-7 and MDA-MB-435S cells with 0.3 mM ATP in the pipette solution. We observed that the currents in MCF-7 cells were almost completely blocked by a specific inhibitor of ATP-sensitive K^{+} channels, glibenclamide, at concentration of 0.5 μM, implying that the outward currents were I_{KATP}. A similar result upon glibenclamide treatment was observed in MDA-MB-435S cells (Fig. 2).

We compared the amplitudes of the I_{KATP} at different test potentials between MCF-7 and MDA-MB-435S cells. The amplitudes of the I_{KATP} in MCF-7 cells were significantly larger than those in MDA-MB-435S cells, when test potentials of −70 to −30 mV were applied ($P < 0.05$). However, at other test potentials, no significant difference in the I_{KATP} was observed between MCF-7 and MDA-MB-435S cells ($P > 0.05$).

Effects of Docetaxel on the I_K and I_{KATP} in MCF-7 Cells

The effect of docetaxel on the I_K in MCF-7 cells was recorded. Results showed that whole-cell I_K was inhibited in a dose-dependent manner by docetaxel added to the extracellular solution (Fig. 3a). When the test potential was

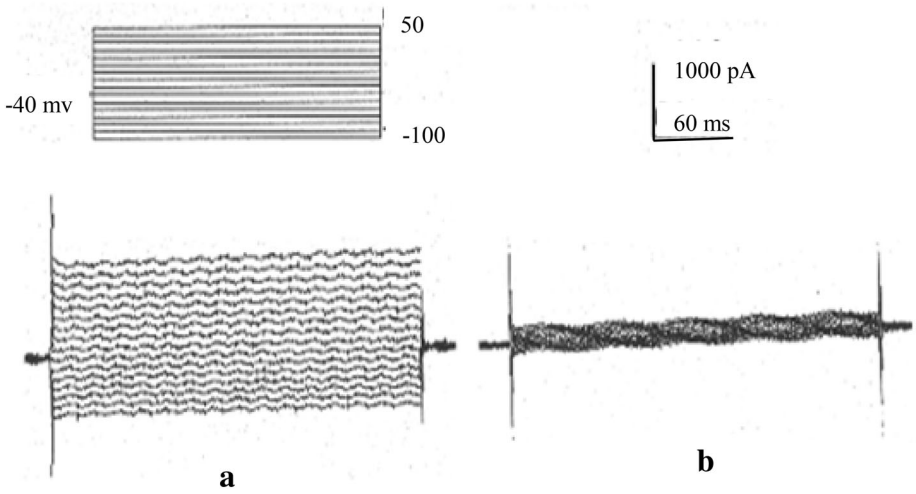

Fig. 2 The effect of glybenclamide on the I_{KATP} in MCF-7 cells. **a** Control; **b** Perfusion with glybenclamide

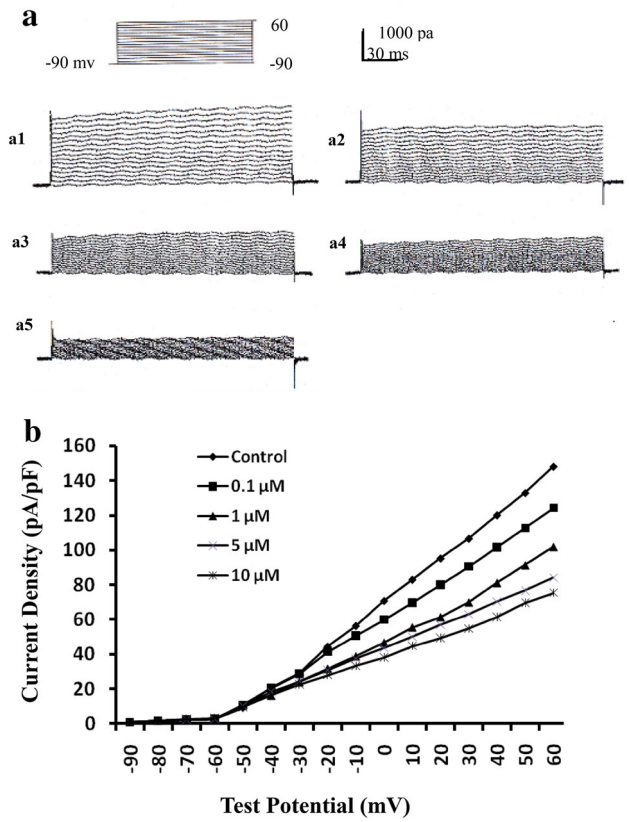

Fig. 3 Effect of docetaxel on the I_K in MCF-7 cells. **a** Whole-cell I_K elicited by a series of 200 ms voltage pulses from −90 to +60 mV in 10 mV increments, from a holding potential of −90 mV. Pulses were applied every 3 s. *a* Control; *b* Perfusion with 0.1 μM docetaxel; *c* Perfusion with 1 μM docetaxel; *d* Perfusion with 5 μM docetaxel; *e* Perfusion with 10 μM docetaxel. **b** Effect of docetaxel on the mean current–voltage relationship of the I_K ($n = 5$ cells)

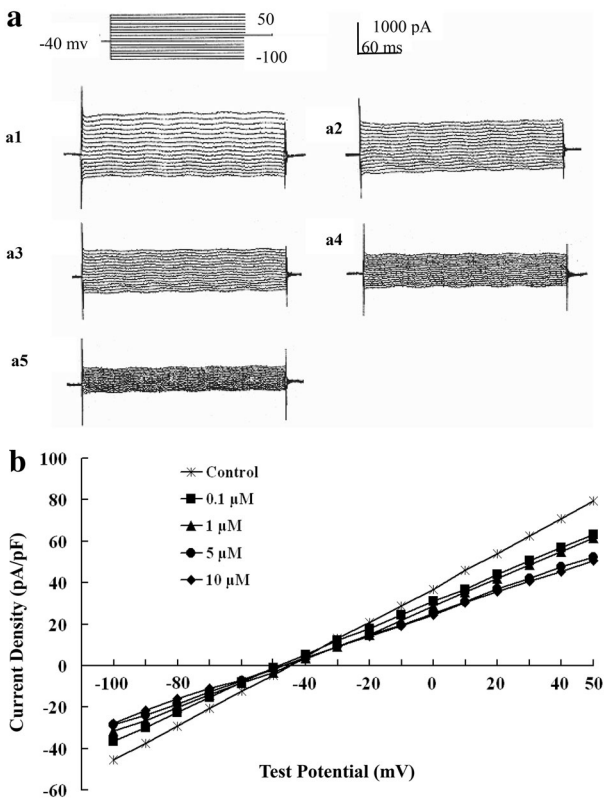

Fig. 4 Effect of docetaxel on the I_{KATP} in MCF-7 cells. **a** Whole-cell I_{KATP} elicited by a series of 300 ms voltage pulses from −100 to +50 mV in 10 mV increments, from a holding potential of −40 mV. Pulses were applied every 3 s. *a* Control; *b* Perfusion with 0.1 μM docetaxel; *c* Perfusion with 1 μM docetaxel; *d* Perfusion with 5 μM docetaxel; *e* Perfusion with 10 μM docetaxel. **b** Effect of docetaxel on the mean current–voltage relationship of the I_{KATP} ($n = 5$ cells)

+60 mV, the I_K reached its peak. At doses of 0.1, 1, 5, and 10 μM, docetaxel blocked the I_K from 124.0 ± 8.4 to 101.7 ± 3.7, 83.9 ± 3.7, and 75.2 ± 9.1 pA/pF, respectively, compared with the control 147.9 ± 7.4 pA/pF ($n = 5$, $P < 0.01$). The respective mean inhibitory rates were 16.1 ± 3.5, 30.2 ± 5.2, 42.5 ± 4.3, and 46.4 ± 9 %

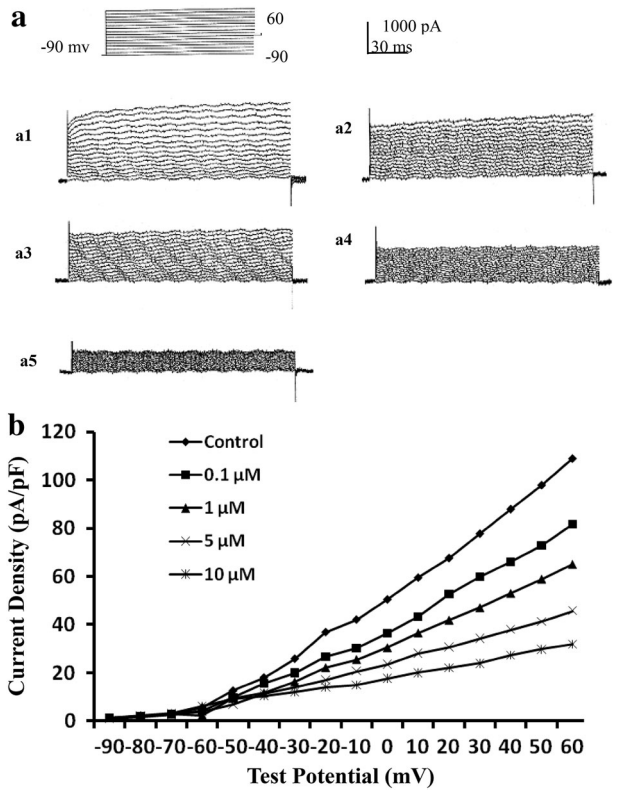

Fig. 5 Effect of docetaxel on the I_K in MDA-MB-435S cells. **a** Whole-cell I_{KATP} elicited by a series of 200 ms voltage pulses from −90 to +60 mV in 10 mV increments, from a holding potential of −90 mV. Pulses were applied every 3 s. *a* Control; *b* Perfusion with 0.1 μM docetaxel; *c* Perfusion with 1 μM docetaxel; *d* Perfusion with 5 μM docetaxel; *e* Perfusion with 10 μM docetaxel. **b** Effect of docetaxel on the mean current–voltage relationship of the I_K ($n = 5$ cells)

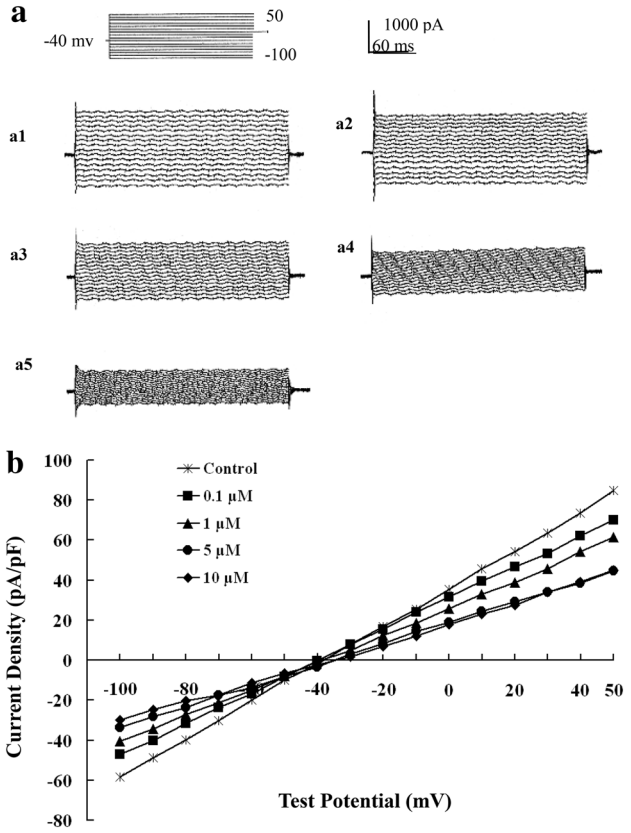

Fig. 6 Effect of docetaxel on the I_{KATP} in MDA-MB-435S cells. **a** Whole-cell I_{KATP} elicited by a series of 300 ms voltage pulses from −100 to +50 mV in 10 mV increments, from a holding potential of −40 mV. Pulses were applied every 3 s. *a* Control; *b* Perfusion with 0.1 μM docetaxel; *c* Perfusion with 1 μM docetaxel; *d* Perfusion with 5 μM docetaxel; *e* Perfusion with 10 μM docetaxel. **b** Effect of docetaxel on the mean current–voltage relationship of the I_{KATP} ($n = 5$ cells)

($n = 5$, $P < 0.05$). Figure 3b shows the dose-dependent effect of docetaxel on the *I–V* curve for the I_K in MCF-7 cells.

At a potential of +50 mV, 0.1, 1, 5, and 10 μM docetaxel reduced the amplitudes of the I_{KATP} from control 79.4 ± 5.7 to 63.2 ± 10.6, 61.4 ± 10.7, 52.3 ± 8.4, and 50.6 ± 6.8 pA/pF, respectively ($n = 5$, $P < 0.05$). The respective mean inhibitory rates were 21.8 ± 11.1, 24.0 ± 11.8, 35.2 ± 15.7, and 36.7 ± 16.4 % ($n = 5$, $P < 0.05$). The docetaxel-mediated, dose-dependent inhibition of the I_{KATP} in MCF-7 cells is shown in Fig. 4a. The effect of docetaxel on the *I–V* curve for the I_{KATP} in MCF-7 cells is shown in Fig. 4b.

Effects of Docetaxel on the I_K and I_{KATP} in MDA-MB-435S Cells

When MDA-MB-435S cells were exposed to an extracellular solution containing docetaxel, whole-cell I_K was inhibited by docetaxel in a dose-dependent manner (Fig. 5a). When the test potential was +60 mV, I_K reached its peak. After treatment with 0.1 μM docetaxel, the I_K was decreased from the control of 109.0 ± 14.1 to 81.7 ± 9.8 pA/pF ($n = 5$, $P > 0.05$). With an increasing dose of docetaxel from 1 to 5 to 10 μM, the I_K was further decreased to 65.5 ± 9.1, 45.7 ± 9.6, and 31.9 ± 7.7 pA/pF ($n = 5$, $P < 0.01$), respectively. The respective mean inhibitory rates for 0.1, 1, 5, and 10 μM docetaxel were 24.1 ± 5.1, 44.2 ± 13.2, 57.5 ± 6.8, and 69.2 ± 6.3 % ($n = 5$, $P < 0.05$). The effect of docetaxel on the *I–V* curve for the I_K in MDA-MB-435S cells is shown in Fig. 5b.

At a test potential of +50 mV, after treatment with 0.1 μM docetaxel, the amplitude of the I_{KATP} in MDA-MB-435S cells was reduced to 70.1 ± 5.7 pA/pF compared with the control of 84.8 ± 4.8 pA/pF ($n = 5$, $P > 0.05$). After treatment with 1, 5, and 10 μM docetaxel, the amplitudes of the I_{KATP} were significantly reduced to 61.5 ± 4.7, 44.5 ± 5.4, and 44.9 ± 5.9 pA/pF ($n = 5$, $P < 0.01$), respectively. The respective mean inhibitory

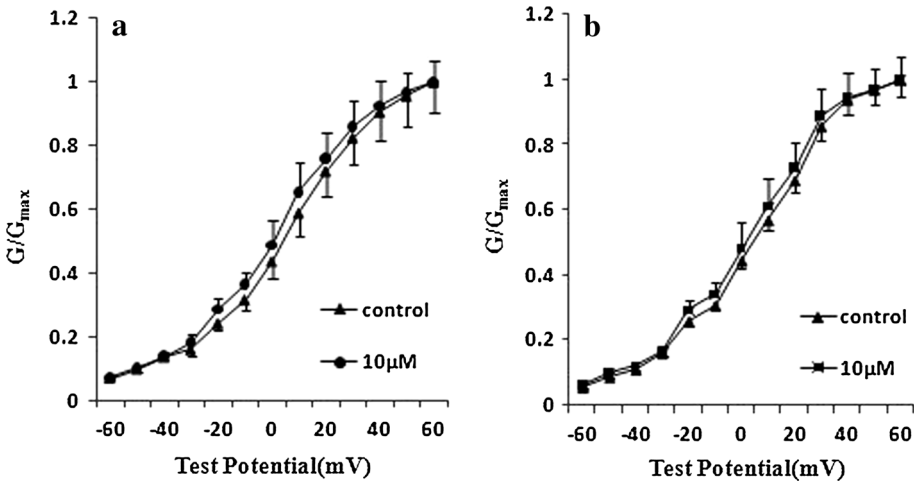

Fig. 7 The *G–V* curve after treatment with 10 μM docetaxel. **a** *G–V* curve in MCF-7 cells. G/G_{max} was calculated as G at different potentials divided by the G_{max} obtained at +60 mV. **b** *G–V* curve in MDA-MB-435S cells ($n = 5$ cells)

rates for 0.1, 1, 5, and 10 μM docetaxel were 17.2 ± 5.6, 26.9 ± 6.2, 47.3 ± 6.5, and 46.8 ± 6.6 % ($n = 5$, $P < 0.05$). Figure 6a shows that docetaxel inhibited the I_{KATP} in MDA-MB-435S cells in a dose-dependent manner. The effect of docetaxel on the *I–V* curve for the I_{KATP} in MDA-MB-435S cells is shown in Fig. 6b.

In our study, we found that the I_{KATP} of MCF-7 might be more sensitive to low-dose docetaxel, but less sensitive to docetaxel as its dose increases. For example, when the highest stimulus voltage was 60 mV, the IC_{50} values of I_K in MCF-7 and MDA-MB-435S cells were 16.54 and 4.42 μM, respectively, based on calculations using SPSS software. However, when the highest stimulus voltage was 50 mV, the IC_{50} values of I_{KATP} in MCF-7 and MDA-MB-435S cells were 182.4 and 9.1 μM, respectively (data not shown).

We also calculated the *G–V* curve of I_K in both MCF-7 and MDA-MB-435S cells in response to 10 μM docetaxel (Fig. 7). G/G_{max} was calculated as *G* at different potentials divided by the G_{max} obtained at +60 mV. Values are presented as means ± SE. The voltage that produces a 50 % effect was calculated by best fit of data points to the Hill equation. The results showed similar *G–V* curves in two types of breast cancer cells, indicating the same channel properties in these cells. Meanwhile, no significant changes in the *G–V* curves were observed after treatment with 10 μM docetaxel, indicating that docetaxel has no effect on the active kinetic curves of I_K in either MCF-7 or MDA-MB-435S cells.

Discussion

In addition to breast cancer cells, prostate cancer cells have also been shown to possess various types of K^+ channels that play important roles in tumorigenesis. Furthermore, differential expression of K^+ channels in prostate cancer cells has been suggested to influence their invasive potential (Hammadi et al. 2012; Maroto et al. 2012). However, whether K^+ channels are associated with the invasive ability of tumor cells in breast cancer remains unknown. In the present study, we evaluated the effects of docetaxel on the I_K and I_{KATP} in the human breast cancer MCF-7 and MDA-MB-435S cell lines. Previous studies revealed the different invasive abilities of these cell lines: MCF-7 cells are weakly invasive, and MDA-MB-435S cells are strongly invasive (Sun et al. 2005). Our data indicate that the I_K and I_{KATP} in MCF-7 cells at the tested membrane voltage were generally much greater than those in MDA-MB-435S cells. This result suggests that the larger currents might generate a potential hyperpolarization of MCF-7 cells, which could correlate with the more negative resting potential and lesser invasive capability of this cell line. In contrast, the smaller amount of K^+ currents in MDA-MB-435S cells produced only small hyperpolarizing currents, which could lead to their more invasive capability. Our results suggest that K^+ channels may play an important role in determining the malignant behavior of breast cancer cells.

Emerging evidence supports that the activation of plasma membrane K^+ channels is involved in the control of tumor cell proliferation (Wonderlin and Strobl 1996; Ouadid-Ahidouch et al. 2000; Wang et al. 1998). Therefore, K^+ channels are considered to be potential pharmacological targets for chemotherapeutic agents. It has been well documented that plasma membrane K^+ channels are required for cell cycle progression at G1 phase (Wonderlin and Strobl 1996). Activation of ATP-sensitive K^+ channels (K_{ATP}) in MCF-7 cells might be responsible for the progression through G1 into the S phase in cell cycle (Klimatcheva and Wonderlin 1999; Strobl et al. 1995). As a consequence, pharmaceutical K_{ATP} inhibitors such as

quinidine, linogliride, and glibenclamide arrest cells in the early G1 phase, leading to the inhibition of cell proliferation (Woodfork et al. 1995; Wang et al. 1998). The effectiveness of K_{ATP} blockers for proliferation inhibition and cell cycle arrest implicates the critical role of K^+ channels in the control of breast tumor growth.

Studies on the I_K involved regulation of tumor cell proliferation have been recently reported and show that I_K blockers such as TEA, 4-AP, and some anticancer agents can inhibit both proliferation and the I_K in a variety of tumor cells (Abdul et al. 2003; Liu et al. 2010).

Recent studies (O'Grady and Lee 2005) showed that epithelial cells express several shaker-type Kv and auxiliary subunit mRNAs and proteins that are typically associated with excitable cells. Such diversity and the constitutive expression of these subunits strongly suggest their function in epithelia. It has been reported that Kv1.1 and Kv1.3 underlie the growth-promoting effect of the I_K in MCF-7 human breast cancer cells (Ouadid-Ahidouch et al. 2000; Abdul et al. 2003). In a comparative study, Kv1.1 K^+ channels were very sensitive to external perfusion with TEA, but Kv1.3 K^+ channels were less sensitive to TEA ($IC_{50} = 10$ mM) (Ouadid-Ahidouch et al. 2000; Grissmer et al. 1994). In terms of specificity of K^+ channels, we tested the sensitivity of the MCF-7 cells to TEA and 4-AP, both of which block voltage-gated K^+ channels. These classical K^+ channel blockers are known to inhibit Kv1.3 K^+ channel currents (Grissmer et al. 1994). At the +60 mV potential, the I_K recorded in MCF-7 cells was reduced by approximately 27 % after extracellular perfusion with 10 mM TEA and by about 46 % when perfused with 10 mM 4-AP. The pharmacological characteristics of the I_K recorded in human breast cancer cells are very similar to those of Kv1.3, a member of the K^+ channel family (Grissmer et al. 1994).

Microtubules are dynamic protein polymers that play an essential role in cell division, maintenance of cell shape, vesicle transport, and motility (Desai and Mitchison 1997). The effects of the drugs on the tubulin cytoskeleton on ion channels have been previously reported (Montalbetti et al. 2007; Galli and DeFelice 1994). Taxanes, as promising anti-cancer drugs associated with spindle and microtubules, are widely used in clinical practice for the treatment of human tumors including ovarian, cervical and endometrial, breast, gastric, and non-small-cell lung cancer. It has been reported that taxanes bind to a pocket in beta-tubulin, on the microtubule's inner surface, leading to inhibition of the microtubule depolymerization process (Smoter et al. 2011).

Docetaxel (or Taxotere) is a clinically well-established anti-mitotic chemotherapy medication that is approved for clinical use by the United States Food and Drug Administration, primarily for the treatment of breast, ovarian, prostate, and non-small cell lung cancer. The anti-neoplastic mechanism underlying docetaxel's action depends on its ability to bind tubulin and excessively stabilize microtubules (Fitzpatrick and Wheeler 2003). Our previous studies reported the effect of docetaxel on growth inhibition in MCF-7 and MDA-MB-435S cells (Sun et al. 2005). To gain a better understanding of the ionic mechanism underlying the inhibition of cancer cell proliferation, we investigated the effect of docetaxel on K^+ currents in breast cancer cell lines. To this end, we examined the whole-cell I_K and I_{KATP} in MCF-7 and MDA-MB-435S cells as well as the effects of docetaxel on the I_K and I_{KATP} in both cell lines. Our study showed that docetaxel attenuated the I_K and I_{KATP} in a dose-dependent fashion, indicating that blockage of K^+ channels may contribute to mechanisms underlying the anticancer action of docetaxel. Although our results were obtained from the raw cells using a previous version of the software (pCLAMP 5.5.1), the effects of the drugs and inhibitors were obvious, and the data are reliable. We believe that the issue of noise in our study does not impair our conclusion related to the effects of docetaxel, because we have repeated the same experiments under the same conditions at least three times, obtaining very similar results in each experiment. Our findings suggest a novel approach to cancer treatment based on the combination of docetaxel and other promising inhibitors of K^+ channels. We expect that this novel cancer therapy will have a greater therapeutic effect than either docetaxel or K^+ channel inhibitors alone.

In summary, our results reveal the dose-dependent inhibitory effects of docetaxel on whole-cell I_K and I_{KATP} in MCF-7 and MDA-MB-435S cells, identifying the mechanisms of the antiproliferative action of docetaxel.

References

Abdul M, Santo A, Hoosein N (2003) Activity of potassium channel-blockers in breast cancer. Anticancer Res 23:3347–3351

Desai A, Mitchison TJ (1997) Microtubule polymerization dynamics. Annu Rev Cell Dev Biol 13:83–117

Dyrager C, Wickström M, Fridén-Saxin M, Friberg A, Dahlén K, Wallén EA, Gullbo J, Grøtli M, Luthman K (2011) Inhibitors and promoters of tubulin polymerization: synthesis and biological evaluation of chalcones and related dienones as potential anticancer agents. Bioorg Med Chem 19:2659–2665

Fitzpatrick FA, Wheeler R (2003) The immunopharmacology of paclitaxel (taxol), docetaxel (taxotere), and related agents. Int Immunopharmacol 3:1699–1714

Galli A, DeFelice LJ (1994) Inactivation of L-type Ca channels in embryonic chick ventricle cells: dependence on the cytoskeletal agents colchicine and taxol. Biophys J 67:2296–2304

Gelmon K (1994) The taxoids: paclitaxel and docetaxel. Lancet 344:1267–1272

Grissmer S, Nguyen AN, Aiyar J, Hanson DC, Mather RJ, Gutman GA, Karmilowicz MJ, Auperin DD, Chandy KG (1994) Pharmacological characterization of five cloned voltage-gated K^+ channels, types Kv1.1, 1.2, 1.3, 1.5, and 3.1, stably expressed in mammalian cell lines. Mol Pharmacol 45:1227–1234

Hammadi M, Chopin V, Matifat F, Dhennin-Duthille I, Chasseraud M, Sevestre H, Ouadid-Ahidouch H (2012) Human ether à-gogo K(+) channel 1 (hEag1) regulates MDA-MB-231 breast cancer cell migration through orai1-dependent calcium entry. J Cell Physiol 227:3837–3846

Hille B (1992) Ionic channels of excitable membranes, 2nd edn. Sinauer Associates, Sunderland

Klimatcheva E, Wonderlin WF (1999) An ATP-sensitive K(+) current that regulates progression through early G1 phase of the cell cycle in MCF-7 human breast cancer cells. J Membr Biol 171:35–46

Leanza L, O' Reilly P, Doyle A, Venturini E, Zoratti M, Szegezdi E, Szabo I (2014) Correlation between potassium channel expression and sensitivity to drug-induced cell death in tumor cell lines. Curr Pharm Des 20:189–200

Liu J, Feng S, Zhang L, Wu Z, Chen Q, Cheng W, Wang SQ, Zou W (2010) Expression and properties of potassium channels in human mammary epithelial cell line MCF10A and its possible role in proliferation. Sheng Li Xue Bao 62:203–209

Maroto R, Kurosky A, Hamill OP (2012) Mechanosensitive Ca(2+) permeant cation channels in human prostate tumor cells. Channels (Austin) 6:290–307

Montalbetti N, Li Q, Wu Y, Chen XZ, Cantiello HF (2007) Polycystin-2 cation channel function in the human syncytiotrophoblast is regulated by microtubular structures. J Physiol 579:717–728

Mound A, Rodat-Despoix L, Bougarn S, Ouadid-Ahidouch H, Matifat F (2013) Molecular interaction and functional coupling between type 3 inositol 1,4,5-trisphosphate receptor and BKCa channel stimulate breast cancer cell proliferation. Eur J Cancer 49:3738–3751

O'Grady SM, Lee SY (2005) Molecular diversity and function of voltage-gated (Kv) potassium channels in epithelial cells. Int J Biochem Cell Biol 37:1578–1594

Ouadid-Ahidouch H, Chaussade F, Roudbaraki M, Slomianny C, Dewailly E, Delcourt P, Prevarskaya N (2000) KV1.1 K^+ channels identification in human breast carcinoma cells: involvement in cell proliferation. Biochem Biophys Res Commun 278:272–277

Ouadid-Ahidouch H, Le Bourhis X, Roudbaraki M, Toillon RA, Delcourt P, Prevarskaya N (2001) Changes in the K^+ current-density of MCF-7 cells during progression through the cell cycle: possible involvement of a h-ether.a-gogo K^+ channel. Recept Channels 7:345–356

Schiff PB, Fant J, Horwitz SB (1979) Promotion of microtubule assembly in vitro by Taxol. Nature 277:665–667

Smoter M, Bodnar L, Duchnowska R, Stec R, Grala B, Szczylik C (2011) The role of tau protein in resistance to paclitaxel. Cancer Chemother Pharmacol 68:553–557

Strobl JS, Wonderlin WF, Flynn DC (1995) Mitogenic signal transduction in human breast cancer cells. Gen Pharmacol 26:1643–1649

Sun T, Li JM, Song ZG, Jia XK, Hu HY (2005) Study on effect of docetaxel on proliferation and invasion of human breast cancer cells. Chin J Cancer Prev Treat 12:429–431

Wang S, Melkoumian Z, Woodfork KA, Cather C, Davidson AG, Wonderlin WF, Strobl JS (1998) Evidence for an early G1 ionic event necessary for cell cycle progression and survival in the MCF-7 human breast carcinoma cell line. J Cell Physiol 176:456–464

Wegman EA, Young JA, Cook DI (1991) A 23-pS Ca2(+)-activated K^+ channel in MCF-7 human breast carcinoma cells: an apparent correlation of channel incidence with the rate of cell proliferation. Pflügers Arch 417:562–570

Wonderlin WF, Strobl JS (1996) Potassium channels, proliferation and G1 progression. J Membr Biol 154:91–107

Woodfork KA, Wonderlin WF, Peterson VA, Strobl JS (1995) Inhibition of ATP-sensitive potassium channels causes reversible cell-cycle arrest of human breast cancer cells in tissue culture. J Cell Physiol 162:163–171

Yasumizu Y, Miyajima A, Kosaka T, Miyazaki Y, Kikuchi E, Oya M (2014) Dual PI3K/mTOR inhibitor NVP-BEZ235 sensitizes docetaxel in castration resistant prostate cancer. J Urol 191:227–234